GA–A24031

POLOIDAL MAGNETIC FIELD MEASUREMENTS AND ANALYSIS WITH THE DIII–D LIBEAM SYSTEM

by
D.M.THOMAS

AUGUST 2002

DISCLAIMER

GA–A24031

POLOIDAL MAGNETIC FIELD MEASUREMENTS AND ANALYSIS WITH THE DIII–D LIBEAM SYSTEM

by
D.M.THOMAS

This is a preprint of an invited paper to be presented at the Fourteenth Topical Conference on High Temperature Plasma Diagnostics, July 8–11, 2002, Madison, Wisconsin, and to be published in the *Proceedings*.

Work supported by
the U.S. Department of Energy under
Contract No. DE-AC03-99ER54463

GENERAL ATOMICS PROJECT 30033
AUGUST 2002

ABSTRACT

For over thirty years, neutral lithium beams have been employed as a localized, noninvasive diagnostic on a variety of plasma experiments worldwide, providing a number of key physics measurements. On DIII-D the LIBEAM diagnostic has been designed to provide precise measurements of the local poloidal magnetic field in the edge region, a parameter of basic importance to understanding the stability of high performance tokamaks. We utilize the Zeeman splitting and known polarization characteristics of the collisionally excited 670.8 nm Li resonance line to interpret local magnetic field components viewed using a closely packed (ΔR ~ 5 mm) array of 32 viewchords. A dual photoelastic modulator/linear polarizer combination serves to amplitude modulate the light in exact correspondence to its input polarization state. Subsequent narrowband spectral filtering using etalons and standard interference filters is used to isolate one of the three Zeeman components, and the polarization state of that component is recovered using a PC-based, multichannel digital lock-in detection system. Edge magnetic pitch angle profiles for a variety of shots have been reconstructed using a small number of chords and detailed analysis of the lockin and d.c. signal levels. Present system performance appears to be limited by etalon performance as well as various broadening mechanisms in the beam that tend to decrease the polarization fraction in the observed component. A careful analysis of this effect and some strategies for improving the measured polarization will be presented.

1. INTRODUCTION

In the quest for fusion power, improving the performance of stable magnetic confinement schemes has been a key scientific issue. Our challenge for the future is to maintain and improve these performance levels on a steady-state (and ultimately economical) basis. In particular, the recent development of the highest performance "advanced" tokamak (AT) modes has relied on the careful crafting of the plasma pressure, current, and rotation profiles, requiring good internal measurements of these parameters with high precision. At present, the maximum attainable pressure of these AT modes of operation is governed by the stability limits of various modes (peeling, ballooning, and kink) rather than by transport considerations.[1,2] In the case of stability of the plasma edge, i.e. the region near the transition between closed and open magnetic field lines, a complex interplay between the sharp pressure gradient and associated large bootstrap current determines the size of the plasma pressure pedestal achieved in the H(igh confinement)-mode as well as the threshold and evolution of edge localized modes (ELMs). To a great extent, this edge behavior sets the confinement and performance of ELMing H-mode discharges. Recent modeling efforts which incorporate the impact of edge current and finite toroidal mode number, n, are able to reconstruct many of the qualitative features of the ELM behavior and pedestal stability for a variety of plasma shapes.[1,2] The development of a specific extended magnetohydrodynamic (MHD) stability code (ELITE)[3,4] that can efficiently handle peeling/ballooning mode coupling, magnetic shear stabilization and current destabilization of peeling modes now allows for detailed comparison with experiment of such important parameters as pressure gradient limits in strongly shaped discharges and radial ELM depth. These comparisons are now limited by the resolution of the various pedestal diagnostics, in particular the lack of an experimental value for the magnitude and shape of the edge current density.

Measurement of the current density profile through the use of the motional Stark effect (MSE)[5] has played a key role in the understanding and development of advanced operational modes. In MSE, the poloidal magnetic field B_θ (and thus the current density via Ampere's Law) is inferred from the measured polarization of the Doppler-shifted D_α emission from an injected hydrogenic neutral beam. The polarization of the Stark-split emission manifold is determined by the electric field in the rest frame of the beam. For tangential views and radial injection, this has historically been identified with the cross product of beam velocity and total magnetic field:

$$E = v_{BEAM} \times B$$

Unfortunately, substantial intrinsic radial electric fields are found to exist in the high gradient regions. In this case (1) generalizes to

$$E = v_{BEAM} \times B + E_r$$

and a simple MSE-style measurement is incapable of distinguishing between the two electric terms without substantial modification of the diagnostic (multiple views, multiple beam injection angles, multiple beam energy components, etc). This is of particular import for studies of the edge bootstrap current where small poloidal magnetic field changes (few %) need to be resolved in the presence of large (~20–100 kV/m) electric fields associated with high-performance H-modes.

This paper discusses the deployment and initial operation of a technique for yielding information on the edge current density j(r), based on the Zeeman effect in the lithium 2S-2P resonance transition. Because of the wide separation of the atomic levels in lithium, there is essentially no Stark mixing and the polarization and splitting of the resonance emission is strictly due to the local magnetic field.[6,7] Another advantage to using lithium is the large oscillator strength associated with the resonance line, and the fact that it has relatively large electron/ion collisional excitation rates for efficiently pumping the transition. This permits measurements to be made with mA-level beam currents in the edge of present day devices.

In Section 2 we briefly review the principle of the technique and describe methods of exploiting it to yield the necessary precision. In Section 3 we cover the various components of the diagnostic system as installed on the DIII-D tokamak. In Section 4 we present results of measurements on DIII-D from the diagnostic along with operational experience. Finally in Section 5, we discuss some improvements that can be implemented to increase the accuracy of measurements using this technique.

2. DIAGNOSTIC PRINCIPLE

In order to determine local details of the magnetic field structure we utilize the Zeeman effect in lithium: in a magnetic field, the spectral line emission is shifted and split due to spin-orbit interaction with the field, with the specific wavelength for each transition being determined by the field strength *B* and the change in magnetic quantum number m.[7] In the case of the lithium 2^2S-2^2P resonance transition (λ_0 = 670.78 nm) the spectral line is essentially split into three Zeeman components with transitions of $\Delta m = 0, +1$, or -1, referred to as π, $\sigma+$ and $\sigma-$ respectively (Fig. 1). The σ components are shifted in wavelength by an amount

$$\Delta\lambda_B = \Delta m(\mu/hc)\lambda_0^2 B$$

for magnetic fields above about 1 T. For the lithium resonance wavelength the shift is 0.021 nm/T. In addition to the spectral behavior, the polarization state of the lines depends on the angle of emission with respect to the magnetic field. For emission perpendicular to B, the π line is linearly polarized parallel to the direction of B and the two σ lines are linearly polarized perpendicular to B. For emission parallel to B, there is no π emission, and the two σ states exhibit circular polarization, with the shorter wavelength $\sigma-$ being left-circularly polarized and the longer wavelength $\sigma+$ being right-circularly polarized.

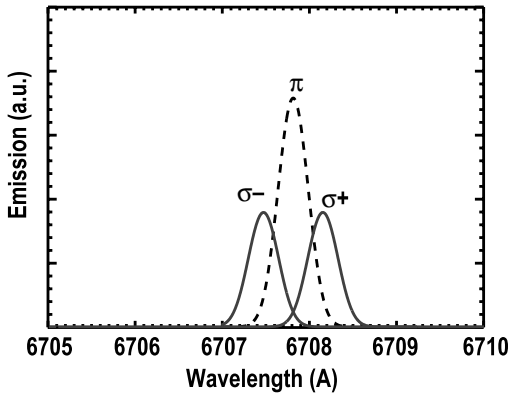

Fig. 1. Lithium line emission profile calculated for a position near the outside midplane of DIII-D for a 2.1 T, 1.86 MA shot. An estimated transverse beam temperature of 1.0 eV was used to calculate the Doppler broadening of the line components. The distance between the two sigma peaks for this example (total B = 1.62 T) is 0.068 nm.

The emission of the [π, $\sigma+$, $\sigma-$] manifold in an arbitrary direction with respect to **B** can therefore be characterized in terms of relative intensity and polarization state, based on the angle of observation with respect to B.[8] In terms of the conventional Stokes parameters [S0,S1,S2,S3] = [total intensity, horizontal linear polarization, linear polarization at +45 deg, right circular polarization],[9] the manifold can be expressed as a function of α, the viewing angle relative to the field and γ, the observed field inclination angle, as follows:

$$\mathbf{I} = [[\mathbf{I}\pi] + [\mathbf{I}\sigma+] + [\mathbf{I}\sigma-]] =$$

$$\mathbf{I}_0 \left[\begin{pmatrix} \frac{\sin^2\alpha}{2} \\ \frac{\sin^2\alpha\cos(2\gamma)}{2} \\ \frac{\sin^2\alpha\ \sin(2\gamma)}{2} \\ 0 \end{pmatrix} + \begin{pmatrix} \frac{1+\cos^2\alpha}{4} \\ -\frac{\sin^2\alpha\cos(2\gamma)}{4} \\ -\frac{\sin^2\alpha\ \sin(2\gamma)}{4} \\ \frac{\cos\alpha}{2} \end{pmatrix} + \begin{pmatrix} \frac{1+\cos^2\alpha}{4} \\ -\frac{\sin^2\alpha\cos(2\gamma)}{4} \\ -\frac{\sin^2\alpha\ \sin(2\gamma)}{4} \\ -\frac{\cos\alpha}{2} \end{pmatrix} \right] \tag{4}$$

Equation (4) is the basis of all methods of inferring magnetic field components, and hence j, from lithium fluorescence measurements. In each case, the goal is to identify ratios of various terms in Eq. (4) in order to deduce the angles α and γ and thereby identify the toroidal, radial, and vertical magnetic field components$\{B_T, B_R, B_Z\}$ through the transformations

$$\cos\alpha = \cos\theta_i \frac{B_z\cos\theta_i + B_R\sin\theta_i}{\left(B_z^2 + B_R^2 + B_T^2\right)^{1/2}} \tag{5}$$

$$\tan\gamma = \frac{B_z\sin\theta_i - B_R\cos\theta_i}{B_T} \tag{6}$$

where θ_i is the view angle with respect to the vertical axis and the poloidal field B_θ is given by

$$B_\theta = \left(B_z^2 + B_R^2\right)^{1/2} \tag{7}$$

Prior analysis techniques have included linear polarization analysis of the collisional fluorescence,[10,11] enhancement and polarization-dependent pumping using a resonant laser to induce fluorescence,[12] line scanning and modulation of the circular polarization to identify parallel field components,[13] and precision line profile intensity measurements to take advantage of the known σ/π variation with field direction.[14] In the present work, we have chosen to determine the field direction by identifying the ratio of circular to linear polarization in one of the σ lines by measuring its ellipticity. This is represented by the ratio of the Stokes parameters

$$\frac{S_3}{\left(S_1^2 + S_2^2\right)^{1/2}} = \frac{2\cos\alpha}{\sin^2\alpha}. \tag{8}$$

3. LIBEAM DIAGNOSTIC DESIGN

The layout of the diagnostic, showing the locations of the lithium accelerator and fluorescence collection system, is shown in Fig. 2. Using a high energy beam has four main advantages. First, it permits measurements to be made well inside the plasma due to the superior beam penetration. Second, beams permit localized measurements by using a transverse viewing geometry with well focussed viewing volumes and in-situ spatial calibrations. Third, beams have a less perturbative effect on the plasma compared to other potential techniques such as pellet injection or laser blow-off. Finally, the achievable Doppler broadening of beam emission is typically much less than that from lithium that has begun equilibrating with the edge plasma, as is found in pellet or laser blow-off clouds.

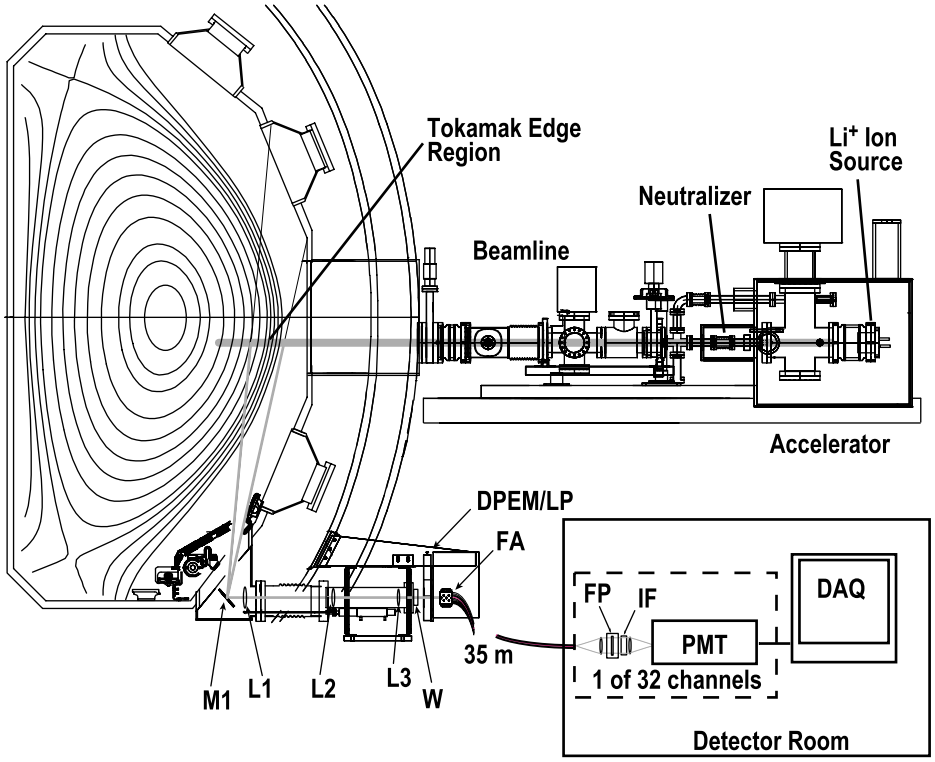

Fig. 2. Neutral lithium beam system and viewing optics system on DIII-D for the Zeeman polarization diagnostic. Beam parameters: 30 keV, 10 mA, 1–2 cm diameter. Radial resolution 5 mm. Lenses L1, L2, L3 and window, W, are SFL6 (low Verdet constant) glass and the polarization-maintaining mirror, M1, has a special coating compatible with extended vacuum exposure and high (350°C) temperature. Dual PEM fundamental frequencies are 23 and 20 kHz. Fiber array (FA) allows up to 32 radial channels to be observed simultaneously.

The system utilizes radial injection and vertical viewing in order to (1) optimize the radial resolution, crucial to unfolding fine-scale detail of the field structure and (2) maximize the sensitivity to the poloidal field component. Many of the hardware development and installation details have been covered in earlier publications,[8,15,16,17] but we review some of the salient features below.

A. Neutral Beam

Because of the relatively small Zeeman splitting, a premium is set on minimizing the Doppler broadening of the lithium line profile in order to minimize the spectral overlap. Since beam temperature is typically a major contributor to line width, we have pursued the development of thermionic ion sources which are capable of extremely low (~0.1 eV) intrinsic ion temperatures. The lithium ion source is based on β-eucryptite, a thermoemissive glass containing isotopically pure ^{6}Li which has been melted into a 5 cm diameter sintered tungsten sponge. When heated, the disk emits ~1 mA/cm^2 when an extraction field is applied. Discs typically last a thousand or more 10 s shots before becoming depleted and requiring recoating. The ion emission from the source disc is accelerated to 30 keV, focussed electrostatically to a diameter of ~1 cm and imaged into the neutralizer region using an electrostatic Einzel lens. The lithium ion beam is neutralized in a 15 cm long sodium vapor cell. The cell is designed along the lines of a heatpipe to help localize the high-density region of the vapor and minimize sodium efflux. This allows us to neutralize the beam in as short a distance as possible, in order to minimize the space charge effects and neutral beam spread. For the energy range used here, neutralization efficiencies of 80%–90% are easily achievable for cell temperatures in the 300°–350°C range. For a high perveance beam it is important to neutralize in as short a distance as possible, in order to minimize the space charge effects and neutral beam spread. Historically, we have left the neutralizer at operating temperature all day; however we are considering pulsing the neutralizer temperature on a shot cycle timescale in order to extend the lifetime of the cell and minimize sodium losses into the accelerator. A remotely insertable wire target can be used to examine beam quality and aiming in the beamline between shots.

B. Optical System

A substantial amount of effort went into the design of the optical system. Most of the details are covered in a companion article.[18] Basically, a four element optical system images the horizontal Li beam onto an array of 3 x 32 1 mm diameter optical fibers, providing 32 spatial channels with 5 mm radial resolution in the plasma. Design features include lenses fabricated from low Verdet constant glass, polarization maintaining mirrors, and an insertable diagnostic polarizer for in-situ measurements. A dual photoelastic modulator (DPEM) is mounted immediately outside of the vacuum window and is used to

modulate the polarization state of the emitted light. A linear polarizer (LP) immediately after the DPEM acts to convert the polarization modulation into amplitude modulation which can then be detected using lock-in techniques, similar to MSE. In-vessel tests of the optics after the 2001 experimental campaign revealed no large systematic variations of the measured polarization due to the various elements, and only minor (~1 mm) spatial shifts of the 32 viewing locations. We believe we have a robust set of optics with good fidelity for polarization determination. Figure 3 shows an expanded view of the edge region for shot 111148, demonstrating the good alignment of the 32 viewchords with the magnetic flux surfaces.

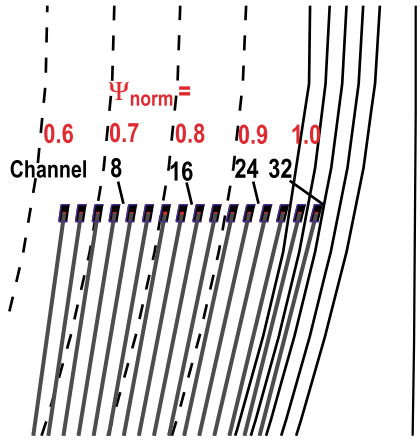

Fig. 3. Edge resolution for Shot 111148. Every other one of the 32 sightlines is shown.

C. Digital Lock-In Analysis

To accurately determine the ratio of circular to linear polarization using modulation techniques requires lock-in measurements at four different frequencies (fundamental and first harmonic of each of the two PEM resonant frequencies). To avoid deploying and tuning 128 separate analog lock-in amplifiers, increases in computer speed and memory have allowed us to pursue true digital lock-in techniques to extract all 4 required frequency components in near real-time. This technique relies on commercial PC/PCI hardware and is scaleable to many channels. Two big advantages of this approach are (1) the elimination of analog noise during the reference mixing and (2) digitizing the PEM reference frequencies allows us to avoid error due to frequency drift. Development of this system is covered in a companion paper.[19] The system is presently capable of processing 8 separate channels simultaneously using a single PC and PCI DAQ board at digitization rates up to 1 MHZ for the full DIII-D shot length.

D. Spectral Filtering Using Etalons

Due to the relatively small separation of the Zeeman states for typical DIII-D discharge conditions, a premium is set on efficient narrow band spectral filtering of the line profile to isolate one of the σ components. A prototype filterscope employing a tilt- and temperature-tuned Fabry-Perot etalon and 1-nm bandpass lithium line filter serves to isolate the proper component, depending on the line broadening that is actually present due to beam thermal spread, finite viewing angle, etc. The filtered intensity is then detected using GaAs

photomultiplier tubes and low noise transimpedance preamplifiers. Because of the slightly different intersection angle of each viewchord with the beam, each desired σ component will exhibit a slightly different (~0.08 Å/channel) Doppler shift. This means each etalon must be individually tuned. The precise shifts were identified on a channel-by-channel basis using a 3/4-m SPEX spectrometer with 1200 groove/mm grating operated in second order. The temperature of each etalon oven was then adjusted to position one of the transmission peaks at the properly shifted wavelength using the same spectrometer. For the 2002 experimental campaign we deployed 7 out of an eventual 32 channels based on this technique.

4. MEASUREMENTS ON DIII-D

By the end of the 2002 run period the system was operating reliably on DIII-D and producing data for a limited number of spatial locations. Figure 4 shows the beam fluorescence collected at several radial locations spanning the range $0.73 < \Psi_n < 1.09$, where Ψ_n is the normalized poloidal flux. These signals were acquired with the etalons removed and are not polarization resolved. The signal levels are reasonably consistent with earlier beam penetration modeling.[8] Numerous spectroscopic measurements of the Doppler-shifted beam emission were taken to assess the effects of operating conditions on the width and position of the line profiles. Although the resolution of the spectrometer (0.48 Å) was not sufficient to resolve the Zeeman structure, the measurements were useful for setting upper bounds on the Doppler broadening and verifying the peak location. Figure 5 shows the measured and calculated line profile for a 2 T, 1.3 MA shot. Accounting for the instrumental function and appropriate Zeeman splitting gives an estimated component FWHM of 0.37 Å, consistent with an equivalent transverse beam temperature of about 3 eV ($\sim 10^{-4}\ E_0$).

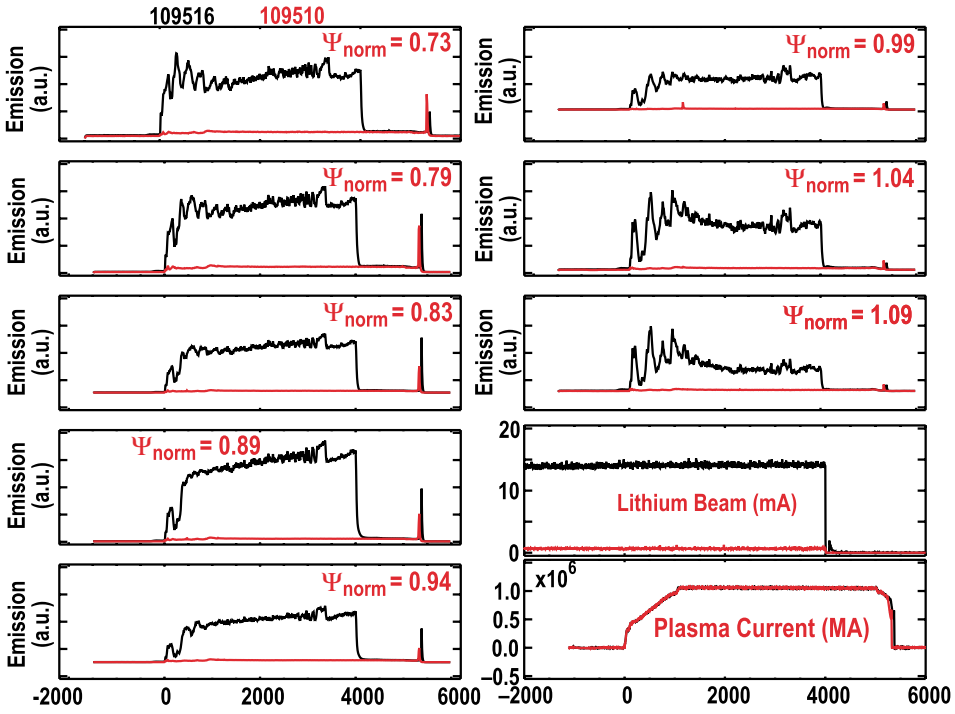

Fig. 4. Lithium beam fluorescence versus radius for DIII-D shot 109516. Also shown (grey) are signals from Shot 109510, an identical shot with no LIBEAM injection for comparison. Plasma density was ~2.5×10^{13} cm^{-3}. Beam is turned off at 4.000 s.

To briefly illustrate the polarimetry data, Fig. 6 shows the calculated pitch angles $\gamma_0(r) = \text{atan}(B_\theta/B_T)$ and some associated plasma parameters on shot 111148, a 1.76 T 1.5 MA Ohmic shot which disrupted around 3460 ms. Flattop is reached around 1230 ms, and an Ohmic H-mode transition occurs around 1400 ms. For this data, channels 1–7 were tuned up for 7 contiguous locations from R = 225.4–228.4 cm, the region just inside the last closed flux surface. Channel 8 had no etalon installed, no net polarization and hence a zero calculated pitch angle. For this discharge, these channels spanned a range in poloidal flux Ψ_n of [0.95–1.05]. Note the edge poloidal field continues to evolve after flattop, until it is essentially clamped after the L-H transition. This behavior is also reflected in the edge magnetic probe and, to a lesser extent the plasma inductance data. The statistical uncertainty in the calculated pitch angles is presently a few tenths of a degree for averaging times in the range 10–100 ms.

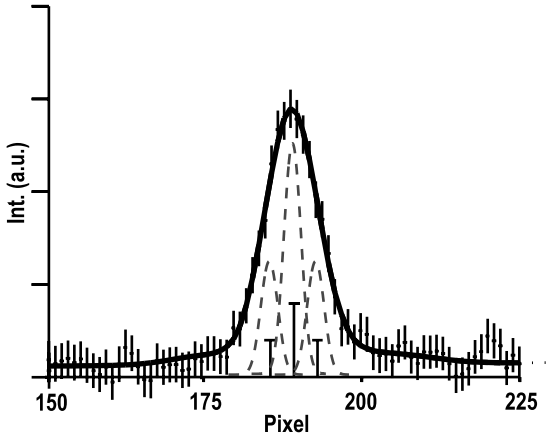

Fig. 5. Measured line profile from SPEX spectrometer for shot 110905, R = 2.239 m. Dotted lines indicate calculated Zeeman triplet with effective temperature of 3 eV.

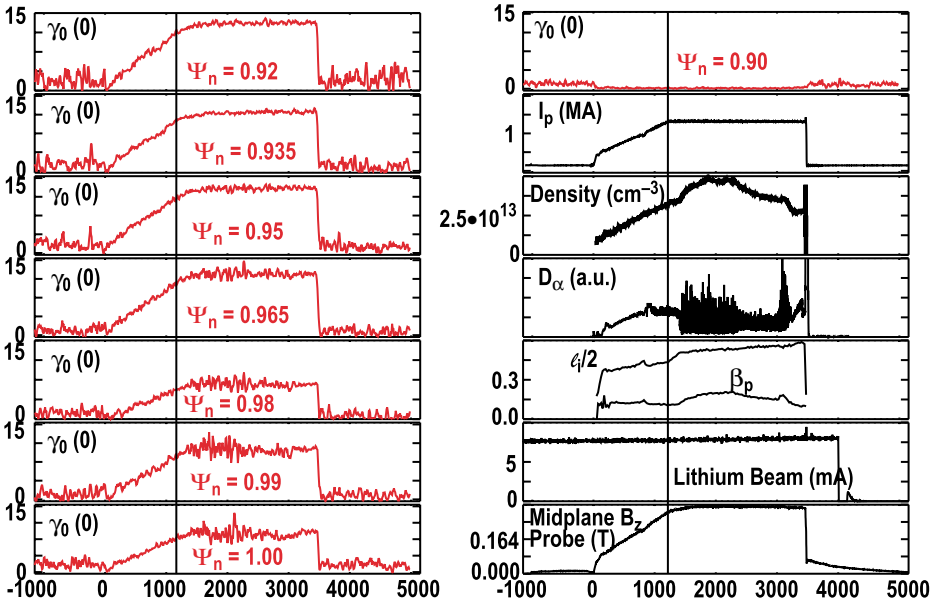

Fig. 6. Calculated pitch angles $\gamma_0 = atan(B_\theta/B_T)$ and plasma parameters for Shot 111148.

5. DISCUSSION

We are still assessing the role of systematic effects on our measurements of B_θ using this technique. A simple but crude test is to compare the measured γ_0 with estimated pitch angles from the equilibrium solver EFIT for our measurement locations, even though these latter are known to be poorly constrained near the separatrix. For all shots examined, EFIT gives values that are systematically higher than the γ_0 calculated from our measurements. Because of non-ideal filtering and the finite Doppler spread for the collected fluorescence, certain fractions of the π and oppositely polarized σ components will bleed through into the detector. This is due to a systematic underestimate of the circular polarization fraction, due to spectral bleed through of a portion of the oppositely polarized sigma line. While excessive energy spread in the beam will eventually increase the overlap of the σ states, we believe the primary contributing factor to the depolarization at present is the inadequate performance of the present etalons. Measurements of the transmission functions using the spectrometer and thermally scanning the etalons while observing a lithium line source indicate the finesse is worse than expected. This results in a substantial transmission of the unwanted σ component when the etalon is properly positioned[18] (Fig. 7).

Modeling the amount of depolarization we would expect for the measured finesse, peak location and beam temperature has been used to estimate correction factors for γ_0. We can accurately account for the additional linear polarization due to the π line by measuring the average intensity S_0 and solving an expanded version of Eq. (8). For the circular bleedthrough due to the oppositely polarized σ, the correction requires an independent calibration of the system. We are trying to determine the best way to improve this situation. Despite the small levels of polarization, the digital lock-in technique is still capable of accurately extracting the polarization components. Because the Zeeman splitting and specific overlap is almost totally determined by B_T, the depolarization factor will barely change during a plasma shot. In order to calibrate the system, we plan to measure the Stokes parameters for a beam–into-gas shot where the magnetic fields, but no plasma, are

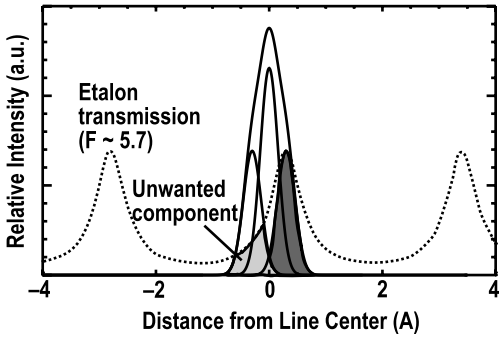

Fig. 7. Depolarization effects due to etalon bleedthrough, using existing finesse and Doppler broadening. Unwanted σ (light grey) is passed by etalon and subtracts from net polarization of desired σ^+ component.

present. In this case it is possible to determine very precise vacuum magnetic equilibria and accurately determine the correction factors.

As a cross check, one can do an alternate calculation of the pitch angle using other terms from Eq. (4). For example, using the ratio of S_1/S_2 provides the tangent of the inclination angle, which can be related to the pitch angle: $\tan\gamma = \tan\gamma_0 \sin\theta$. This can be done trivially using a different combination of the existing lockin voltages. Since both S_1 and S_2 are linear polarization terms, the same depolarization term will occur for both and the ratio will therefore be independent of the exact overlap. Unfortunately, because of the near parallel alignment between our existing view chords and B_θ this is a relatively insensitive test for most DIII-D discharges.

Our results to date demonstrate the capability of making localized measurement of Stokes parameters and calculating magnetic field components in exactly the region desired for comparison with edge stability models. The main remaining issue is improving the measured circular polarization and determining accurate calibration procedures to verify the absolute pitch angle values. In order to increase the rejection of the unwanted σ component, the finesse of the etalons needs to be improved substantially. Modeling indicates a factor of 3 improvement in F would reduce the depolarization from ~30% to 6% or less. Achieving this sort of improvement on surface flatness and pinhole finesse will be challenging but should be possible. Multielement filters having much steeper transmission edges than a single cavity etalon are also being explored. Improving the beam brightness will also help on statistics, and a more parallel beam will give less overlap. Finally, implementing a complimentary set of tangential viewchords gives us the option of measuring the linear ratio S_1/S_2 with much more sensitivity to the magnetic pitch angle, at the cost of decreased radial resolution. These views can then be used to calibrate the overlaps associated with the vertical views, thereby regaining the spatial resolution.

REFERENCES

[1]L.L. Lao, *et al.*, Nucl. Fusion **39**, 1785 (1999).
[2]C.M. Greenfield, *et al.*, Phys. Plasmas **7**, 1959 (2000).
[3]P.B. Snyder, *et al.*, Phys. Plasmas **9**, 2037 (2002).
[4]H.R. Wilson, *et al.*, Phys. Plasmas **9**, 1277 (2002).
[5]F. Levinton, *et al*., Phys. Rev. Lett. **63**, 2060 (1989).
[6]R.D. Cowan, *The Theory of Atomic Structure and Spectra*, (U. California Press, 1981) 498 ff.
[7]H.A. Bethe and E.E. Salpeter, *Quantum Mechanics of One- and Two-Electron Atoms*, (Plenum, 1977) 205 ff.
[8]D.M. Thomas, *et al.*, Rev. Sci. Instrum. **72**, 1023 (2001).
[9]D.S. Kliger, J.W. Lewis, C.E. Randall, *Polarized Light in Optics and Spectroscopy*, (Academic Press, 1990) 75 ff.
[10]K. McCormick, *et al.*, Phys. Rev. Lett. **58**, 491 (1987).
[11]K. Kadota, *et al.*, Rev. Sci. Instrun. **56**, 857 (1985).
[12]W.P.West, D.M. Thomas, J. S. deGrassie, and S.B. Zheng, Phys. Rev. Lett. **58**, 2758 (1987).
[13]L.K. Huang, *et al.*, Phys. Fluids **B2**, 809 (1990).
[14]K. Korotkov, *et al.*, Proc. Workshop on Advanced Diagnostics for Magnetic and Inertial Fusion, Varenna, Italy (2001).
[15]D.M. Thomas, A.W. Hyatt, and M.P. Thomas, Rev. Sci. Instrum. **61**, 3040 (1990).
[16]D.M. Thomas, Rev. Sci. Instrum. **66**, 806 (1995).
[17]D.M. Thomas, *et al.*, Proc. Workshop on Advanced Diagnostics for Magnetic and Inertial Fusion, Varenna, Italy (2001).
[18]T.N. Carlstrom, *et al.*, these proceedings.
[19]D. Finkenthal, *et al*., these proceedings.

ACKNOWLEDGMENTS

This work was performed under the U.S. DOE Contract DE-AC03-89ER51114. The installation and commissioning of this diagnostic has relied on a substantial fraction of the DIII-D group. The efforts of J. Kulchar, D. Hoyt , S. DiPaoli, J. Lynch, A. Bozek, J. Peavy, and J. Robinson are particularly appreciated. Frequent discussions with A.W. Leonard, T.H. Osborne, T.N. Carlstrom, and K.H. Burrell, and numerous others helped to refine our understanding of the measurement. The use of the CER group's spectrometer for the line measurements and etalon tuning was deeply appreciated. The continuing support and encouragement of T.S. Taylor and R.D. Stambaugh is also gratefully acknowledged.